Tropical East–West Circulations During the Northern Winter

T. N. KRISHNAMURTI, MASAO KANAMITSU, WALTER JAMES KOSS[1] AND JOHN D. LEE
Dept. of Meteorology, Florida State University, Tallahassee 32306

(Manuscript received 13 October 1972, in revised form 13 February 1973)

ABSTRACT

In this paper we present the geometry and intensity of the mean east–west circulation during the northern winter. We show that near the equatorial latitudes two pronounced regions of divergent mass outflow in the upper troposphere are found near the convective regions over the northwestern part of South America and Indonesia. The intensity of the east–west circulation is shown to be of the order of 1 m sec^{-1} which is comparable to the intensity of the Hadley circulation. The divergent streamlines are shown to be important for the maintenance of the three waves of the subtropical westerly jet in the Northern Hemisphere, and are shown to exhibit asymptotes of convergence in the regions of mid-oceanic upper tropospheric troughs over the tropical southern oceans. Kinetic energy exchanges for a tropical belt 15S to 15N at 200 mb are expressed as a function of zonal wavenumber. Results for northern summer and winter seasons are compared. We find that wave interactions with the mean zonal flow differ in the two seasons. During the northern summer the long waves (wavenumbers 1 and 2) transfer kinetic energy to the zonal flow which in turn transfers kinetic energy to the short waves (wavenumbers 6, 7 and 8). During the northern winter the opposite occurs: long waves receive kinetic energy from the zonal flow while short waves transfer kinetic energy to the zonal flow.

Finally, we evaluate the generation of eddy kinetic energy by the mean east–west circulations during the two seasons. We show that the east–west circulations are thermally direct, i.e., there is a generation of eddy kinetic energy, on horizontal scales >10,000 km. We furthermore find that this generation during the northern summer is about an order of magnitude larger than for the northern winter.

1. Introduction

This is a sequel to a recent paper on east–west circulations during the northern summer (Krishnamurti, 1971b; henceforth referred to as I) in which it was shown that 1) the intensity of the circulations is comparable to that of the Hadley-type circulation; 2) the circulation is thermally direct; 3) there is a generation of kinetic energy by these east–west overturnings of mass; and 4) this circulation is distinctly different from the so-called Walker circulation, which is a southern extension of the more vigorous east–west circulation.

The primary reason for this study is to point out that the divergent east–west and Hadley-type circulations as depicted by the 200-mb data are quite different during the summer and winter seasons. As a consequence, major seasonal differences are to be expected in the energetics of the large-scale circulation systems. The divergent east–west circulations are henceforth referred to only as the east–west circulations.

As in I, we decompose a velocity vector **V** into the rotational part $\mathbf{V}_\psi$ and a divergent part $\mathbf{V}_\chi$, i.e.,

$$\mathbf{V}=\mathbf{V}_\psi+\mathbf{V}_\chi, \tag{1.1}$$

where, for the purpose of this paper, the quantities are time means for a season (3 months). A time-mean velocity potential χ is defined by

$$\mathbf{V}_\chi=-\nabla\chi. \tag{1.2}$$

We define the intensity of the Hadley and east–west circulations by the respective relations,

$$I_H=-\frac{1}{L}\oint\frac{\partial\chi}{\partial y}dx, \tag{1.3}$$

$$I_E=-\frac{1}{(y_2-y_1)}\int_{y_1}^{y_2}\frac{\partial\chi}{\partial x}dy, \tag{1.4}$$

where L is the length of a latitude circle and y_1 and y_2 are the southern and northern limits of a tropical channel of interest. Note that I_H varies along y, while I_E varies along x. A proper geometrical depiction of the Hadley cell can be presented on a meridional vertical plane while that for the east–west cell would more appropriately be a zonal plane. The velocity potential χ is a seasonal mean obtained from a solution of the equation

$$\nabla^2\chi=-\nabla\cdot\mathbf{V}, \tag{1.5}$$

where **V** is the seasonal mean horizontal velocity vector and is assumed to be known. In this study there are no east–west boundaries as the latitude band of interest encompasses the globe, and χ is set to zero at the north and south boundaries.

[1] Present affiliation: The National Hurricane Research Laboratory, NOAA, Miami, Fla.

Data for the northern winter of 1969 were obtained from the National Meteorological Center, while those for the northern summer of 1967 were from Krishnamurti and Rodgers (1970). The quality of the data for the northern winter is somewhat questionable since they were not collected for research purposes. Nevertheless, we felt that it was appropriate to use operational data for the northern winter season since tropical circulations on daily maps are known to contain, primarily, very long wave features associated with the subtropical jet stream of winter (Krishnamurti, 1961). The summer circulation, on the other hand, is known to contain a myriad of smaller scale eddy motions (Krishnamurti and Rodgers, 1970; Krishnamurti, 1971a). We are aware that lack of data could account for the absence of smaller scale systems in winter.

In the following sections we examine a number of interesting problems which relate to the east–west circulation during northern winter season.

TABLE 1. List of symbols.*

I_E	intensity of the east–west circulation
I_H	intensity of the Hadley circulation
$\bar{K}$	zonal mean total kinetic energy
K_E	eddy kinetic energy
K_L	kinetic energy of long waves (wavenumbers 1 and 2)
K_Z	kinetic energy of the mean zonal flow
$\mathbf{k}$	unit vertical vector
L	length of a latitude circle
$\bar{P}$	zonal mean total potential energy
P_E	eddy potential energy
P_L	potential energy of long waves
P_Z	potential energy of the mean zonal flow
T	time mean temperature
u	time mean zonal velocity component
v	time mean meridional velocity component
$\mathbf{V}$	time mean total velocity vector
$\mathbf{V}_\chi$	time mean rotational velocity vector
$\mathbf{V}_\psi$	time mean divergent velocity vector
ω	time mean vertical velocity component
χ	time mean velocity potential
ψ	time mean streamfunction
y_1, y_2	northern and southern limits of the latitude band of interest

* An overbar is used to denote zonal means. Symbols without bars represent time means which are averages over a 3-month period.

2. Velocity potential during the northern winter season

If the isopleths of the velocity potential χ are parallel to latitude circles, then there would be no east–west circulations. On the other hand, if the isopleths of χ are parallel to longitude meridians, then Hadley-type circulations would be absent. In I, the authors showed that the isopleths of χ during northern summer were more circular over the region of the summer monsoons, and concluded that the streamlines of the divergent part of the wind were more radial than either purely meridional or purely zonal. As a consequence, they inferred that the intensities of the Hadley and east–west type circulations were comparable. A relation between the isopleths of χ and $\nabla^2\chi$ may be seen from the following (see Table 1 for a list of symbols).

If $\mathbf{A}$ stands for a vector with components A_x and A_y, such that

$$A_x=-\frac{\partial\xi}{\partial x}, \tag{2.1}$$

$$A_y=\frac{\partial\xi}{\partial y}, \tag{2.2}$$

then

$$\mathbf{k}\cdot\nabla\times\mathbf{A}=\nabla^2\xi. \tag{2.3}$$

In natural coordinates we may also write

$$\mathbf{k}\cdot\nabla\times\mathbf{A}=-\frac{\partial A}{\partial n}+\frac{A}{R}, \tag{2.4}$$

where $A=(A_x^2+A_y^2)^{\frac{1}{2}}$, n is normal to the isopleths of A, and R is the local radius of curvature of the A isopleths.

If $\mathbf{A}$ is the velocity vector $\mathbf{V}$, we may identify ξ with the streamfunction ψ and speak of the shear and curvature vorticities. We can provide a similar interpretation for the divergent part of the velocity field. Let

$$\nabla^2\chi=-\frac{\partial B}{\partial n}+\frac{B}{R}, \tag{2.5}$$

where

$$B=(B_x^2+B_y^2)^{\frac{1}{2}}, \tag{2.6}$$

$$B_x=-\frac{\partial\chi}{\partial y}, \tag{2.7}$$

$$B_y=\frac{\partial\chi}{\partial x}. \tag{2.8}$$

Thus, we may interpret the regions of large divergence to have an analogous relation to the curvature and shear of the χ isopleths as regions of large vorticity have to the curvature and shear of the ψ isopleths.

Fig. 1 shows the isopleths of the velocity potential during northern winter. The geometry is quite different from that for northern summer; here isopleths of χ are more parallel to the latitude circles and the Hadley-type vertical overturnings are evidently stronger. This is in agreement with the findings of Oort and Rasmussen (1970) who showed that the intensity of the Hadley cell is stronger during northern winter than in northern summer. There are two regions where maximum values of χ are found in the equatorial latitudes, and streamlines of the divergent part of the motion field emanate from these regions. (As may be noted from the preceding discussions, regions of maximum divergence, i.e., regions of maximum $-\nabla^2\chi$, do not necessarily coincide with regions of maximum χ). The two centers of χ maxima

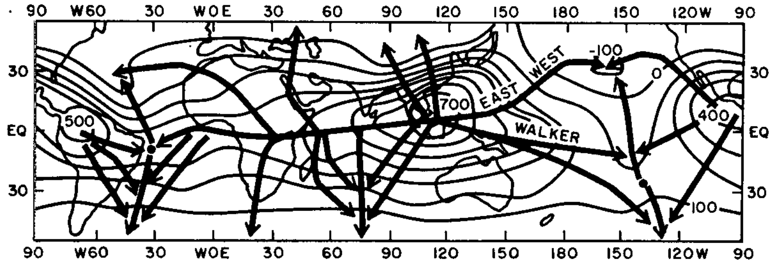

FIG. 1. Isopleths of the winter mean velocity potential χ at 200 mb, and streamlines of the divergent part of the wind shown with arrows. Units for χ, 10^4 m^2 sec^{-2}; interval of analysis, every 100 units. Note the two regions of χ maxima over the equatorial latitudes and the asymptotes of streamline convergence over the southern oceans.

are located over the northwestern part of South America and the equatorial rainbelt near Borneo. An asymptote of diffluence in the streamline field may be noted all along the equatorial belt. The location of the "Walker circulation" over the western Pacific near the equator is nearly at the same position as was noted during northern summer in I. The streamlines of the divergent motions converge near 30N over the Pacific and Atlantic Oceans directly above the sea level, subtropical high pressure belts. The strongest divergent motions are found over eastern Asia where the local contribution to the Hadley circulation $(-\partial\chi/\partial y)$ is largest. This is also a region where the strongest winds at 200 mb during northern winter were noted by Krishnamurti (1961).

A schematic diagram of the vertical cells based on Eq. (1.4) for the two seasons is shown in Fig. 2. The results here are averaged between the equator and 30N for the northern summer and between 15S and 15N for the northern winter. The reason for the different choice of latitude belts is dictated by the active regions of the

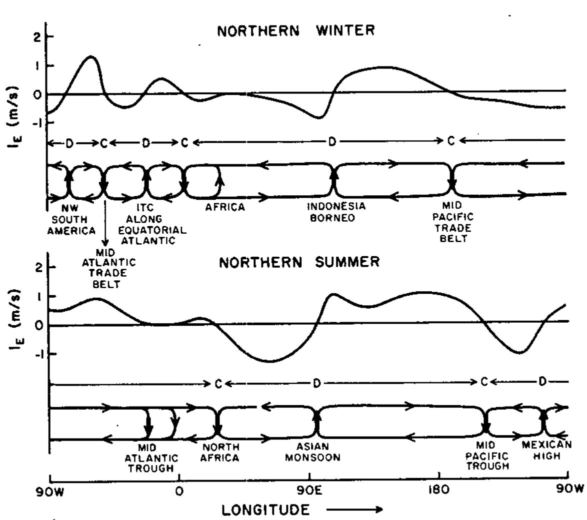

FIG. 2. Intensity of east–west circulation, I_E, at 200 mb, as a function of longitude, and a schematic diagram of east–west cells on mass continuity. C and D indicate regions of upper tropospheric convergence and divergence, respectively.

east–west circulations. Of interest in this figure are the locations of rising and sinking motions. Also shown is the intensity of the 200 mb east–west circulation (m sec^{-1}); it is of interest that the intensity of this circulation is comparable to that of Hadley-type circulations. It should also be noted that the intensity of the east–west circulation during the northern summer is somewhat stronger than during the northern winter. The letters marked C and D in Fig. 2 represent upper tropospheric convergence or divergence, based entirely on the calculations of I_E at 200 mb. The remaining geometry of the vertical cells is inferred from mass continuity. It is quite possible that these cells have tilts in the vertical plane, but we do not feel that presently available data in the tropics at several levels are sufficient to indicate this.

3. Rotational part of the wind during the northern winter at 200 mb

Isopleths of the streamfunction ψ for the northern winter are shown in Fig. 3. These should be compared with the corresponding figures for northern summer presented in I. Westerlies dominate the subtropics of the Northern Hemisphere and the subtropical jet stream of winter is evident in the regions where $|\mathbf{k}\times\nabla\psi|$ is large (see also Krishnamurti, 1961). The three waves of the subtropical jet stream have three regions of maximum velocity, off the southeastern United States, south of the Mediterranean Sea, and off the coast of Japan. The divergent part of the motion field shows pronounced Hadley-type north–south overturnings in these regions.

4. Regions of active convection during the northern winter

Fig. 4 shows mean January cloudiness (mean of January 1966 and January 1967) from Sadler (1970b). Sadler's use of the okta classification of cloud cover pertinent in this figure is based on the following: oktas 5 and 6 are mostly covered, oktas 3 and 4 are mostly open, and oktas 1 and 2 are open, i.e., $\leqslant 20\%$ cloudiness. The three regions of most interest are the northwestern

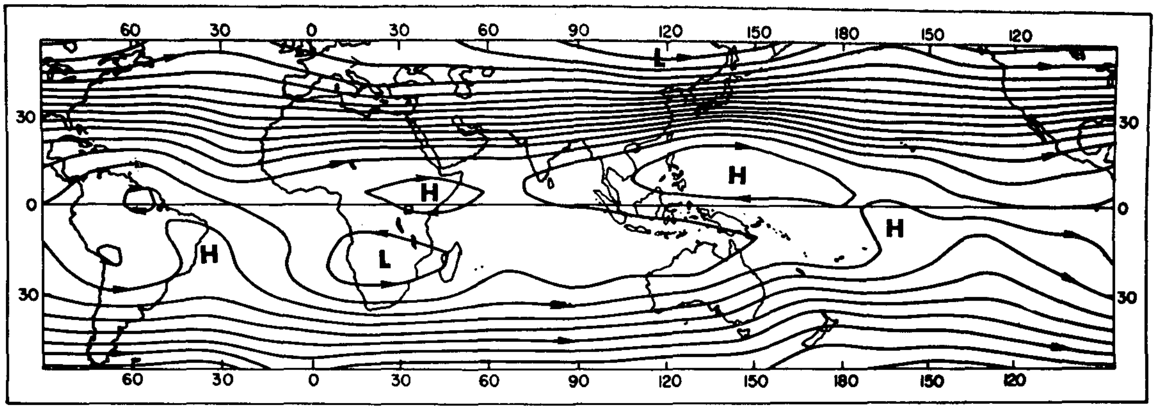

FIG. 3. Isopleths of winter mean streamfunction ψ at 200 mb. Units for ψ, 10^5 m^2 sec^{-2}; interval of analysis, every 50 units.

part of the South American continent, equatorial Africa, and the region around Indonesia and Borneo. In these regions maximum cloud cover values are around 5–6. These are three of the most active convective regions along the ITCZ during the northern winter season. Convective rainfall in these regions over the northwestern part of South America and over the regions of Indonesia are known to exceed 100 inches during the winter season. The strong correlation between these regions and the centers of the upper tropospheric velocity potential maximum is perhaps more than a coincidence. During the northern summer, Krishnamurti (1971b) noted an upper tropospheric velocity potential maximum in the vicinity of the rain belt of the southwest monsoons. An interesting difference between the northern summer and winter is the following. During the northern summer, active monsoon rainfall and the χ maximum are both located close to 20N, with the region of large upper level divergence being located near the Tibetan anticyclone. During the northern winter, on the other hand, no similar large anticyclonic circulations (Fig. 3) are found in the vicinity of the maximum values of χ or $-\nabla^2\chi$. The apparent reason for this is that active convection and upper divergence are both large closer to the equator during the northern winter. The upper tropospheric pressure field does not adjust to the divergence field in the same way as it would at 20° or 30° latitude. This problem relates to the dynamic adjustment of the pressure and the divergent motion field in the vicinity of the equator. Results on this problem will be presented in a subsequent paper.

The important observational result here is that climatologically active convective regions are very well correlated with large-scale regions of upper divergence ($-\nabla^2\chi$). As shown in Krishnamurti (1971b), and by Kanamitsu *et al.* (1972), the geometry of the χ isopleths have important implications for the tropical east–west circulation and long-wave dynamics.

5. Tropical mid-oceanic troughs in northern winter over the southern oceans

North of the equator, during summer, one finds two major, quasi-stationary upper troughs (near 200 mb) over the Atlantic and Pacific Oceans (Aspliden *et al.*, 1966; Sadler, 1967). The geometry of these mean summer upper troughs may be noted also in Krishnamurti and Rodgers (1970), and in Krishnamurti (1971a, b). We attributed the presence of these mid-oceanic troughs to the dynamical effects of vigorous east–west circulations. During northern winter the voluminous work of Sadler (1970a) showed that similar mid-oceanic tilted troughs do exist over the tropical southern Pacific. The mean flow for December 1969 for the entire tropics was calculated for this purpose and is shown in Fig. 5. We note three upper troughs over the Southern Atlantic, Indian and Pacific Oceans. The tilt of the troughs is from northwest to southeast over the Pacific and Indian Oceans. Westerly angular momentum flux is directed toward the summer pole. We feel that these troughs over the southern oceans form due to long-wave vertical overturnings in somewhat an analogous manner as in the northern summer (Krishnamurti, 1971a). Con-

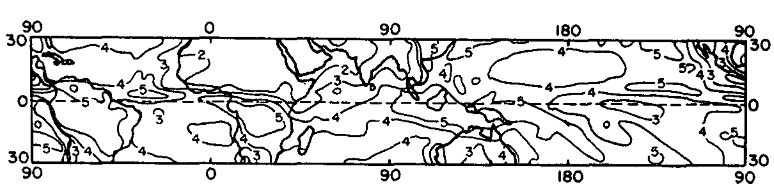

FIG. 4. Cloudiness (oktas) for winter (after Sadler, 1970b).

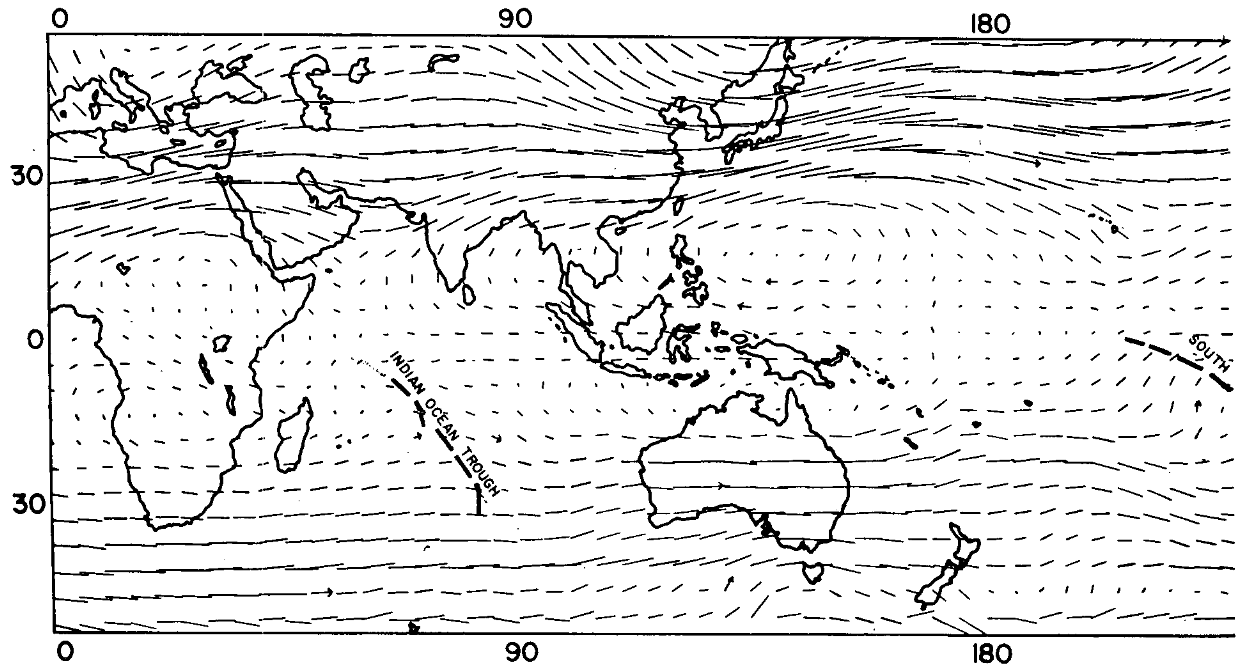

FIG. 5. Total mean motion field at 200 mb for December 1969. The wind vector scale is indicated. Note the mid-oceanic troughs over the southern oceans during northern winter.

vergence is not as strong in the vicinity of the southern oceans as compared to the northern summer mid-oceanic troughs, but we do note asymptotes of convergence of the streamlines of the divergent part of the wind near the southern oceanic troughs. The three principal regions of convection near the equator during northern winter (Fig. 4) must account for the three waves of the subtropical jet stream in the Northern Hemisphere and the three mid-oceanic troughs of the Southern Hemisphere. *Thus, the regions of convection provide a major link between the flows in the two hemispheres*. This link is manifested by the geometry of the velocity potential. The importance of wavenumber 3 was illustrated by Krishnamurti (1961) for the Northern Hemisphere and by Van Loon (1972) for the Southern Hemisphere.

At this stage of our work we have certainly not explained this interhemispheric coupling of long waves, but we hope that the observational evidence presented here will open up interesting enquiries in the future.

6. Kinetic energy exchanges between zonal flows and eddies

During northern summer wavenumber 1 transfers significant amounts of kinetic energy to zonal flows (Kanamitsu *et al.*, 1972), The kinetic energy exchanges during northern winter are generally opposite to those found for northern summer. The tropical belt considered here extends from 15S to 15N at the 200-mb level (Fig. 6). The procedure for calculation is identical to that given in Kanamitsu *et al.* We believe that this is explained as follows. The leading term in the kinetic energy transfer between eddies and zonal flows at a latitude circle is given by

$$\langle K_E \cdot K_Z \rangle = -\bar{u}\frac{\partial \overline{u'v'}}{\partial y}. \tag{6.1}$$

This expresses a correlation between the mean zonal flow $\bar{u}$ and the convergence of flux of westerly momentum. No attempt was made to assess the relative contributions of the rotational and divergent parts of the wind to Eq. (6.1). An overbar indicates zonal mean, and the velocity components are time means for a season (3 months). During northern summer over the tropical belt between 15S and 15N, $\bar{u}<0$, and for long waves (wavenumber 1) we note a large divergence of flux of westerly momentum, i.e., $-(\partial/\partial y)\overline{u'v'}/<0$, the latter result being a consequence of very pronounced tilt of the long waves (Krishnamurti, 1971a). During northern winter the mean zonal flow in the belt 15S to 15N is westerly (although there is a small belt near the equator where it is easterly). The long waves have a pronounced tilt from northwest to southeast over the southern oceans; thus, we again find that there is a flux of westerly momentum directed toward the summer pole (the South Pole). As a consequence, we find that the exchange $\langle K_E \cdot K_Z \rangle<0$ for long waves. We also note that $\langle K_E \cdot K_Z \rangle>0$ for shorter waves (wavenumbers 4, 6 and 7) during northern winter, again opposite to that for the northern summer. A spectral analysis of the

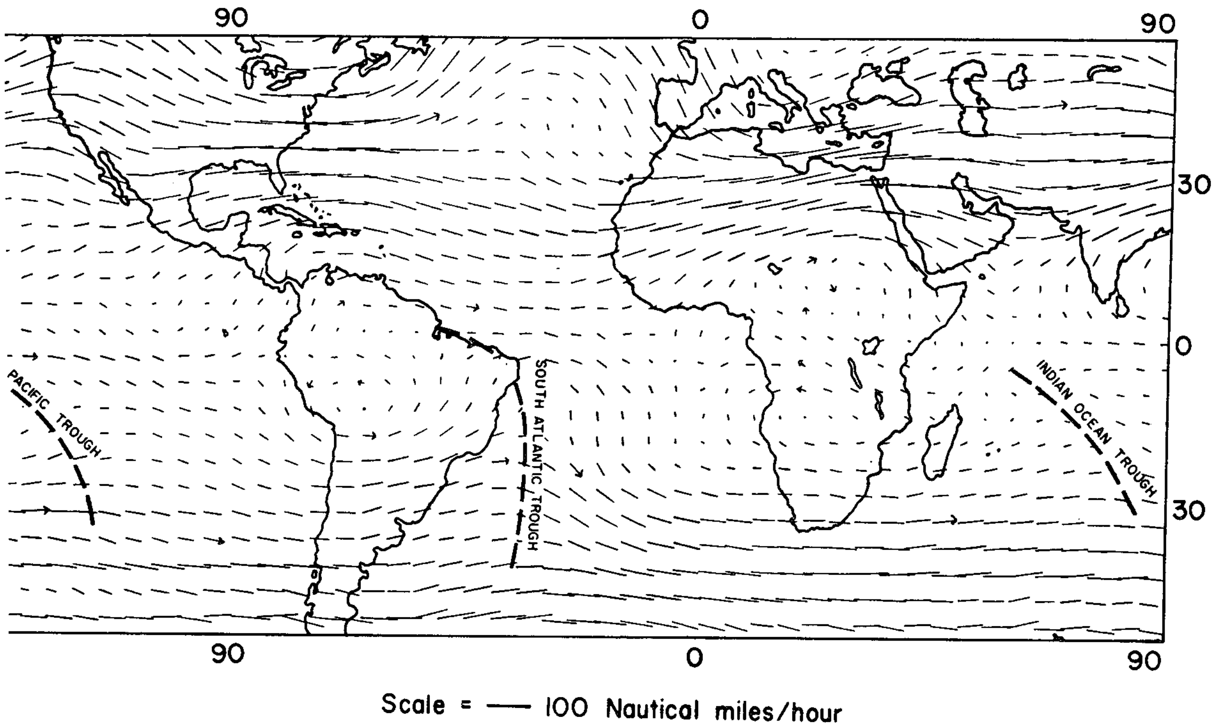

FIG. 5. (*continued*).

motion field during northern winter shows large variances in wavenumbers 1–3. Since the subtropical jet stream of the northern winter has three pronounced waves, we are thus led to conclude that the three waves of the subtropical jet stream receive energy via energy transfers from the zonal flows.

Typical values of some of the energy exchanges are presented in the concluding remarks.

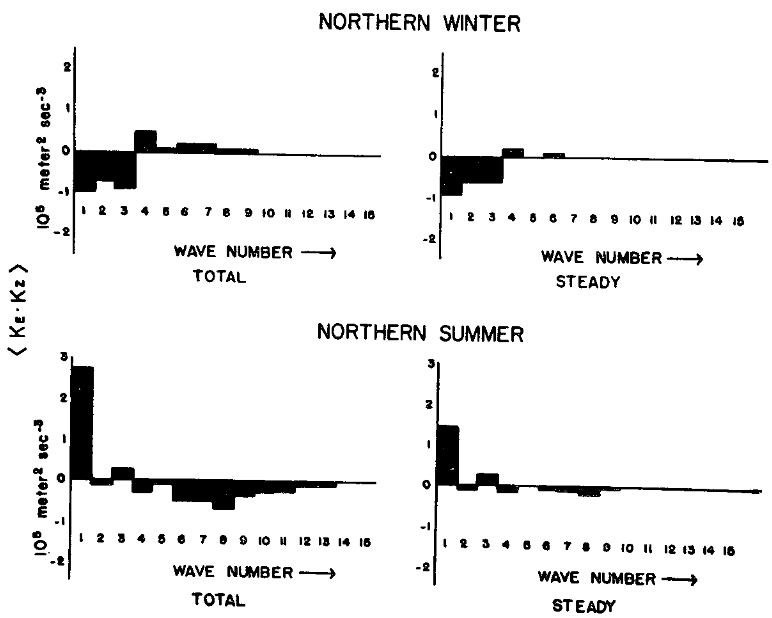

FIG. 6. Kinetic energy exchange between eddies and zonal flows as a function of zonal wavenumber. Results apply to the tropical belt 15S to 15N. Calculations were performed on daily data for three months for respective seasons.

TABLE 2. Values of 300-mb zonally averaged temperature $\bar{T}$, vertical velocity $\bar{\omega}$, and the correlation $\overline{\omega' T'}$ between vertical velocity and temperature, during northern winter and summer seasons.

	Northern winter			Northern summer		
	4.9S	Equator	4.9N	15N	20N	25N
$\bar{T}$(°K)	242.1	242.1	242.0	242.4	242.3	242.0
$\bar{\omega}$ (10^{-5} cb sec^{-1})	−1.0	−1.7	−1.7	−1.46	−1.52	−1.28
$\overline{\omega' T'}$ (10^{-5}K cb sec^{-1})	0.24	−0.40	−0.69	−1.14	−4.2	−7.16

In conclusion, we attribute the reversal of the energy exchanges (Fig. 6) between the two seasons primarily to the reversal in the direction of the mean zonal flows and not to a change in the convergence of flux of the westerly momentum.

7. Generation of eddy kinetic energy by mean east–west circulations

The generation of eddy kinetic energy is an important and somewhat less understood problem over the tropics.

In a zonally asymmetric distribution of east–west vertical circulation, if the rising branches of the circulation are relatively warm compared to the sinking branch, then we should find a generation of eddy kinetic energy on the scale of these vertical circulations. Although eddy kinetic energy on a certain scale can be generated by various transient processes, in the following we shall only compare the generation by the seasonal mean east–west circulations. The computations refer to the equation

$$\langle P_E \cdot K_E \rangle = -\frac{R}{g} \int_x \int_y \int_p \frac{\overline{\omega' T'}}{p} dx dy dp, \qquad (7.1)$$

where ω' is the deviation from the zonal mean vertical velocity $\bar{\omega}$, and ω is the time-mean (3 months) vertical velocity which is related to the time-mean velocity potential χ via the mass continuity equation, i.e.,

$$\nabla^2 \chi = -\frac{\partial \omega}{\partial p}. \qquad (7.2)$$

The boundary condition for (7.2) is $\omega = 0$ at $p = 100$ mb. The integral in (7.1) was evaluated over 1-mb depths centered at 300 mb for 10° wide zonal strips; computations were made for northern winter and summer seasons.

The active latitude belts of the east–west circulations vary seasonally. During northern winter the active latitude belt is near the equator (Fig. 1), while during northern summer the active belt is found near 20N (Krishnamurti, 1971b). With this in view, we present some parameters in Table 2. The zonally averaged temperature in the active belt at 300 mb is approximately −31C during both seasons. The upward branch of the Hadley cell is evident in the active belt as indicated by mean upward vertical motions of the order of 1.5×10^{-5} cb sec^{-1} at 300 mb.

The sign of the correlation $\overline{\omega' T'}$ is negative, implying a generation of eddy kinetic energy by the standing vertical circulations, or east–west circulations. The generation of eddy kinetic energy by the thermally direct east–west circulation is found to be an order of magnitude larger during northern summer as compared to northern winter. From the calculations performed in this and related studies (Kanamitsu *et al.*, 1972), we note the following:

Typical generation of eddy kinetic energy per unit mass $[-(R/p)\overline{\omega' T'}]$ by standing east–west circulation at one level, i.e., 300 mb	$\sim 10 \times 10^{-5}$ m^2 sec^{-3}
Typical value of energy exchange between zonal flow and eddies at one level, i.e., 200 mb	$\sim 3 \times 10^{-5}$ m^2 sec^{-3}
Typical value of nonlinear energy exchange between "waves and waves" at one level, i.e., 200 mb	$\sim 1 \times 10^{-5}$ m^2 sec^{-3}

Thus, we note that the generation of eddy kinetic energy by the standing east–west circulation is significant.

8. Concluding remarks

During northern winter there are three major regions of active convection near the equator. These are located over the northwestern part of South America, over central Africa, and around Borneo and Indonesia. In the vicinity of these regions large-scale low-level convergence and upper level divergence are manifested by the velocity potential minima and maxima, respectively. The presence of three such regions of velocity potential maxima, in the equatorial belt at 200 mb, gives rise to an asymmetric geometry for the Hadley-type vertical overturnings. Where these Hadley-type overturnings are more pronounced over the Northern Hemisphere, we find three associated regions of velocity maxima of the subtropical jet stream: over the southeast coast of the United States, south of the Mediterranean sea, and off the east coast of Asia near Japan (Krishnamurti, 1961). The zonal asymmetry of the velocity potential furthermore appears to be important for the maintenance of three mid-oceanic troughs over the southern oceans. We thus view the three regions of equatorial convection as an interhemispheric connecting link for the quasi-stationary long waves in the subtropical latitudes.

Weak mean zonal westerly flow of the upper troposphere over the regions of convection is found to lose energy to the eddies (around wavenumber 3), i.e., $\langle K_Z \cdot K_L \rangle > 0$, Furthermore. we view the Hadley-type overturning as an energy source for the kinetic energy of the mean zonal flows during northern winter, i.e.,

$$\langle P_Z \cdot K_Z \rangle > 0.$$

Asymmetries such as the tilt of long waves result in the removal of westerly momentum away from the tropical belt; thus, they weaken the mean zonal westerlies and strengthen the eddies. Zonal asymmetries of thermally direct vertical overturnings furthermore suggest that

$$\langle P_L \cdot K_L \rangle > 0.$$

Fig. 7 is a schematic diagram of the gross energetics for the long waves during northern winter. The following explicit computations were performed from the 1969 data to confirm the direction of the energy exchanges as indicated by arrows in this figure:

$$\langle \bar{P} \cdot \bar{K} \rangle > 0 \quad \text{at 200 and 300 mb}$$
$$\langle P_L \cdot K_L \rangle > 0 \quad \text{at 200 and 300 mb}$$
$$\langle \bar{K} \cdot K_L \rangle > 0 \quad \text{at 200 mb.}$$

The exchange $\langle \bar{P} \cdot P_L \rangle$ was not computed. Maps of the temperature and motion fields suggest that eddies transport heat down the thermal gradient at higher levels, i.e., sensible heat is advected poleward by the quasi-stationary long waves. A similar diagram for the northern summer is given in Fig. 8.

The computations also showed that the east–west calculations are thermally direct and active near the equator during northern winter, and near 20N during northern summer. Vertical motions show the upward branch of the Hadley cell in the active belt, and the generation of kinetic energy by the thermally direct east–west circulations is found to be an order of magnitude greater during northern summer than during northern winter.

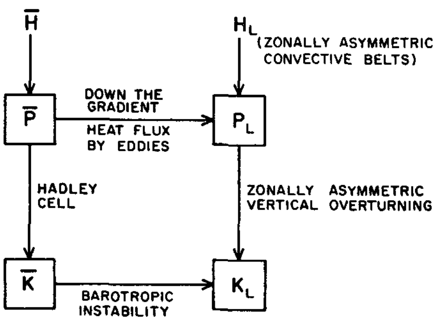

FIG. 7. Schematic energy exchanges for northern winter between long waves and zonal motions in the tropical belt 15S to 15N.

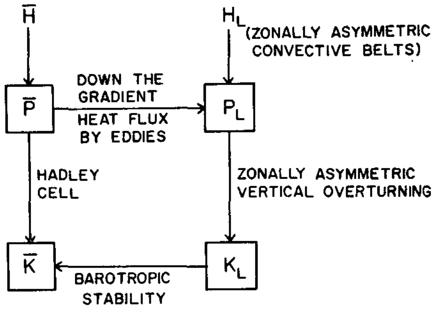

FIG. 8. Schematic energy exchanges for northern summer between long waves and zonal motions in the tropical belt from the equator to 30N.

Acknowledgments. This work was carried out in part in a graduate laboratory course in tropical meteorology. The assistance of several students was important for its completion.

Financial support was provided by the Atmospheric Science Section of the National Science Foundation, under Grant GA-17822, and by the Department of Defense, under Grant DAAB-07-72-C0062.

Computation time was provided by both the Florida State University and by the National Center for Atmospheric Research which is supported by the National Science Foundation.

REFERENCES

Aspliden, C. I., G. A. Dean and H. Landers, 1966: Satellite study, Tropical North Atlantic, 1963. Tech. Rept., Grant WBG 58, Florida State University, Tallahassee.

Kanamitsu, M., T. N. Krishnamurti and Colin Depradine, 1972: On scale interactions in the tropics during northern summer. *J. Atmos. Sci.*, **29**, 698–706.

Krishnamurti, T. N., 1961: The subtropical jet stream of winter. *J. Meteor.*, **18**, 172–191.

——, 1971a: Observational study of the tropical upper tropospheric motion field during the Northern Hemisphere summer. *J. Appl. Meteor.*, **10**, 1066–1096.

——, 1971b: Tropical east–west circulations during the northern summer. *J. Atmos. Sci.*, **28**, 1342–1347.

——, and E. B. Rodgers, 1970: 200 millibar wind field June, July, August 1967. Tech. Rept. No. 70-2, Florida State University, Tallahassee, 118 pp.

Oort, A. H., and E. M. Rasmussen, 1970: On the annual variation of the monthly mean meridional circulation. *Mon. Wea. Rev.*, **98**, 423–442.

Sadler, J. C., 1967: The tropical upper tropospheric trough as a secondary source of typhoons and a primary source of trade wind disturbances. Final Rept. No. AFCRL-67-0023, University of Hawaii, Honolulu, 48 pp.

——, 1970a: Mean monthly upper-tropospheric winds of the central and eastern Pacific from aircraft reports. Tech. Rept. No. 327, Hawaii Institute of Geophysics, Honolulu, 6 pp.

——, 1970b: Mean cloudiness and gradient level charts over the tropics. Tech. Rept. No. 215, Air Weather Service (MAC), U. S. Air Force, 63 pp.

Van Loon, H., 1972: Winds in the Southern Hemisphere. *Meteor. Monogr.*, **13**, No. 35, 87–111.